BME-ETT laborkomplexumban gyártott a NyHL-ek fémezéseinek és forrasz ötvözetek korróziós vizsgálata

Kutatási jelentés

Introduction

One of the key reliability issues of the electronics technology is carry about the solder joints testing. Usually, the different failures can lead back to the not adequate physical properties (e.g. wetting behaviour, mechanical strength, etc.) of the solder alloy and/or the not adequate applied technological processes (e.g. reflow temperature profile), which have to be improved. This challenge was updated in 2006, with the introduction of lead-free solder alloys governed by the RoHS directive of EU [1]. Due to the lead-free limitations, different solder types such as near-eutectic Tin-Silver, Tin-Copper, and Tin-Zinc alloys were produced as replacement for Tin-Lead solder materials. Furthermore, solders with more alloying elements, such as (Tin-Silver-Copper, Tin-Zinc-Silver, Tin-Zinc-Indium) and/or (Tin-Zinc-Silver-Aluminum, Tin-Silver-Bismuth-Copper, Tin-Indium-Silver-Antimony) were also investigated as replacements for Pb-free types [2]. While, the different qualifying studies of the Pb-free solder alloys are even active topics [3] and one of the issues is carry about humidity induced failures, like electrochemical corrosion [4, 5]. Different results were also published related to novel Pb-free solder alloys in terms of reliability topics, such as solderability [6], intermetallic layer (IML) investigation [7], shear force tests [8], wetting investigations [9] or (solid state physics) migration tests [10]. On the other hand, the investigations of humidity induced failures (like corrosion) of Pb-free solder alloys are not deeply addressed in the scientific publications. In our former publication [11], various micro-alloyed Pb-free solders tested in terms of corrosion resistance using electroanalytical tests. In that study [11] different Pb-free solder alloys (four micro-alloyed and a Sn96.5Ag3Cu0.5 alloy as reference) were compared using potentiodynamic polarisation tests. During polarisation tests, the sample (working electrode) is scanned from a cathodic polarisation state, and after reaching the corrosion potential (Ecorr) it begins anodic polarisation. When the sample reaches the passivation potential, if possible a passivation film begins to form on the surface and the current density at this point is called the critical current density (Icrit). After this point the corrosion current density begins to drop to a much lower value. When a compact passivation film is formed on the surface, the corrosion current density becomes stable and this current density is called the passivation current density (Ip). After this point the corrosion remains at the same level and the potential of the sample will increase continually until the potential reaches the breakdown potential. At this point the passivation film begins to break and pitting corrosion happens to the material underneath, resulting in an increase of the corrosion current density. For comparison the I_{crit} or I_p parameters were used, hence these parameters have relative high current densities, and therefore they are very characteristic for the electrochemical corrosion processes, such as ion formation, current exchange, etc. According to the results in [11], one of the micro-alloyed samples showed the highest susceptibility for corrosion, while the other micro-alloyed solder alloys showed a relatively better corrosion parameters compared to SAC305. In this study, we try to find answer for the different corrosion behaviour between the Pb-free solder alloys. For this purpose, new samples were prepared to repeat the polarization (corrosion) tests. The formed corrosion products were investigated by Scanning electron microscopy (SEM) and energy dispersive spectroscopy (EDS) methods. The morphology and the chemical composition of the different corrosion products were investigated.

Experimental

A special Pyrex tube was applied with 60 mm height and the inner diameter of the tube was about 20 mm. In the first phase, Pb-free solder materials were heated up to 160 °C to separate the flux and solder. In the second phase, the solder material has reached the melting point and Pb-free solder paste was reflowed. A vacuum chamber and Ar gas were also used to control void formation and oxidation of the surface, respectively. After cooling down, the formed solder samples (Fig. 1) were brushed using a (240 and 4000 grain sizes) silicon-carbide papers to reach flat and "oxide-free" surfaces.

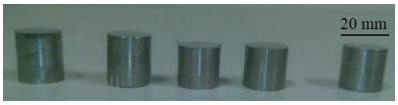

Fig. 1 Cylinder shaped solder samples for polarization tests

The elemental composition of the samples can be seen in Table 1. The commonly applied Sn96.5Ag3Cu0.5 was selected as reference and the other four types were μ-alloyed Pb-free solder alloys. Furthermore, it is known that fluxes and even the so called "No clean" fluxes are not fully evaporate during the reflow soldering process and therefore they will act as contaminations, which can have a significant impact on the reliability from the corrosion point of view [12]. To ensure the same effect of fluxes, the same flux type was selected in all cases.

Table 1 Compositions of the solder alloys in wt%

Sample	**Sn**	**Ag**	**Cu**	**Bi**	**Sb**	**Ni**
I.	96.5	3	0.5			
II.	98.95	0.3	0.7			0.05
III.	98.4	0.8	0.7	0.1		
IV.	98.45	0.8	0.7			0.05
V.	90.95	3.8	0.7	3	1.4	0.15

To study the electrochemical corrosion behaviour of the μ-alloyed solders, electroanalytical investigations were made to reach polarization curves using a VoltaLab PGZ301 polarization equipment (See Fig. 2: 5). Figure 2 shows the drawing of the measuring platform for potentiodynamic polarisation test, where the counter electrode is platinum (1), working electrode is the cylinder shaped sample made by lead-free solder alloy (2), and a saturated calomel electrode as a reference electrode (4) with Luggin capillary bridge (3) connected to the test medium, which is 3.5 wt.% NaCl solution (6). The active area of the working electrode was about 100 mm^2.

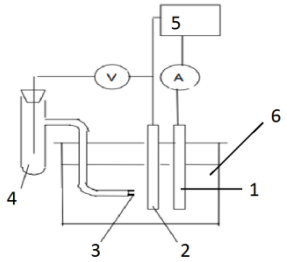

Fig. 2 Schematic of the measuring platform for potentiodynamic polarization test

Before starting the electroanalytical investigations, the optimal scan range was determined. Therefore, a relative wide potential range between -2000 and 3000 mV was measured firstly and finally the active range was fixed from -1500 mV to +1500 mV. Every electroanalytical tests were started on a fixed potential value (– 1500 mV) to ensure an "oxide-free" surface. Furthermore, the positions of the electrodes are also fixed (40 mm distance between working and platinum electrode). In order to obtain the corrosion parameters, the applied scan rate was fixed on 60 mV/min and three measurements were carried out in each cases as well.
After the polarization tests SEM investigations were carried out to study the morphology of the corroded surfaces and the corrosion depth applying cross-sectional samples. To identify the chemical composition of the corrosion products, EDS method was also used.

Results

Polarization tests of the solder alloys

As it was mentioned the polarization test (reported in [11]) was repeated to ensure the reproducibility. Table 2. contains the main results of the polarization test. According to the critical current density (Icrit) values, the following corrosion ranking was established in [11] (II. is the best):

II. > III. > IV. > I. (Ref) > V. (1)

On the other hand, according to the passivation current density (Ip) values, the following corrosion can be established (II. is the best):

II. > IV. > III. > I. (Ref) > V. (2)

Both results are very characteristic for the corrosion properties and they are in good agreement as well.

Table 2 Corrosion parameters of the solder alloys [11]

Sample	E_{corr} [mV]	I_p [mA/cm^2]	I_{corr} [uA/cm^2]	I_{crit} [mA/cm^2]
I.	-590	**3.16**	0.14	**120.72**
II.	-569	**2.5**	0.083	**98**
III.	-597	**2.89**	0.011	**107.66**
IV.	-568	**2.65**	0.024	**112.62**
V.	-570	**9.83**	0.84	**158.27**

Based on the ranking results in Table 2, it can be stated that sample V. showed the lowest corrosion resistance compared to the other solder alloys including SAC305 (reference) as well. Furthermore, the above mentioned corrosion results were also supported by the current polarization test results. However, further study was needed to explain why sample V. was the most critical from the corrosion point of view. Therefore, SEM-EDS investigations were carried out on the corroded products.

SEM-EDS study of the corrosion products

As a first step, after polarization tests the corroded surfaces were observed by SEM. However, there were only little differences between the surface morphology of the solder alloys. Furthermore, similar fishbone-like dendrites were also formed in all a cases. A typical fishbone-like structure can be seen in Figure 3 and Figure 4 shows a typical corroded surface.

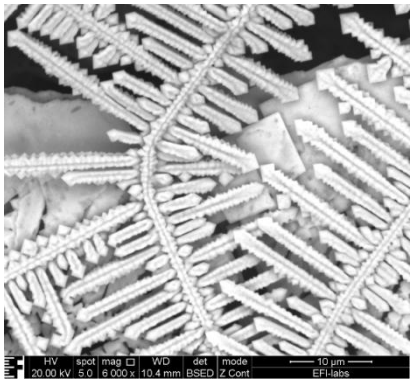

Fig. 3 An example for a fishbone-like dendrite in case of sample V

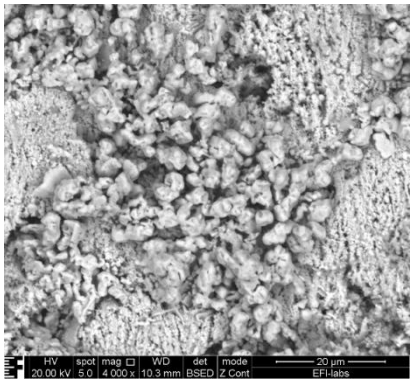

Fig. 4 An example for a corroded surface in case of sample V

On the second step, the cross-sectional samples were investigated by SEM to compare the corrosion depths. For the corrosion depth calculation the same magnifications were used in all cases. An example for depth measuring can be seen in Figure 5.

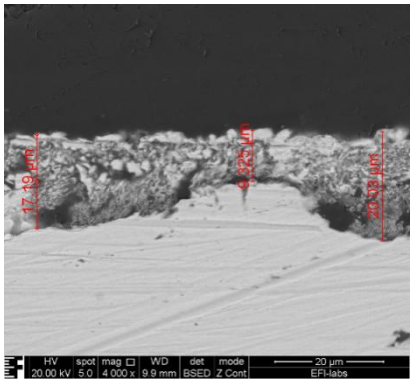

Fig. 5 An example for a corroded depth measure using cross sectional samples and measurement levels for EDS data.

At least five depth measurements were carried out in all cases. The average values and deviations of the corroded depth measurement are presented in Figure 6.

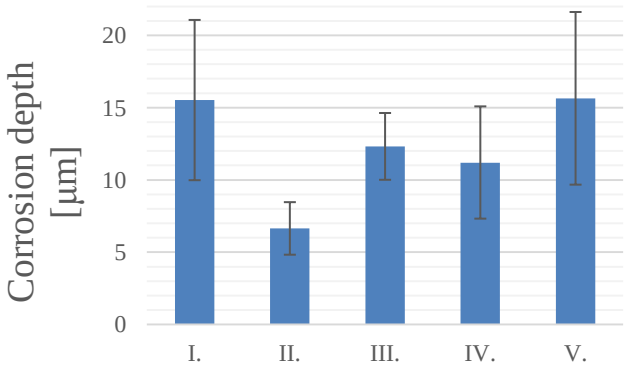

Fig. 6 Corrosion depths of the different solder alloys

Discussion

According to the corrosion depth measurements, sample II. was the best, while sample V. and sample I. showed the lowest resistance against corrosion. These results (Fig. 6) are also in good agreement with the presented corrosion rankings (eq. 1 and 2). Interestingly, according to the EDS result a huge volume of Ag (about 10 wt%) was found in the corrosion product in case of sample V. and SAC305. That was one of the most important difference compare to the other samples. Furthermore, in the case of sample V, around 2.6 wt% Bi was also detected in the corrosion product. So, probably the Bi content of the solder alloy has an impact on the corrosion resistance as well. Table 3 shows the summarized EDS results obtained from three different areas: See Figure 5 and Table 3.

Table 3 EDS results (in wt%) of the solder alloys after polarization test (*A*: surface of the corroded product, *B*: In the middle of the corroded product, *C*: interface between corroded product)

Sample		*C*	*O*	*Cu*	*Ag*	*Sn*	*Bi*	*Na*	*Cl*
I.	***A***	2.3	8.6	0.8	**4.2**	7.5		5	4
	B	17.9	5.7	1.9	**11.6**	63			
	C	20.8	5.8	0.4	1.5	71.5			
II.	***A***	2.4	3.8	0.5		90.8		0.7	1.1
	B	34.1	11.4	1.2	0.1	53.1			
	C	42.9	13.2	1.3		42.6			
III.	***A***	2.1	10.5	0.6	1.5	82		2.4	1
	B	22.4	5.3	2.5	0.1	69.7			
	C	43.9	10.9	1.7	0.4	43.1			
IV.	***A***	1.2	2.6	0.5	1.2	94		0.4	0.1
	B	27.5	8.4	1.2	0.6	62.4			
	C	27.4	8.2	0.1	0.9	63.4			
V.	***A***	1.4	2.8	0.3	**6.9**	84.4	**2.4**	0.9	1
	B	14.6	6.5	1.6	**13**	62	**2.3**		
	C	12.1	5.4	1.7	**10.1**	67.5	**3.3**		

It is known that the bismuth additions can significantly depressed the melting temperature of Sn–Ag-based lead-free solder alloys [13, 14]. Further advantage of adding bismuth into Sn–Ag system solder is the improvement of solder wetting/spreading behaviour [15, 16]. It was also already shown that bismuth and silver can have a significant impact on the corrosion properties in case of Sn-based solder alloy in NaCl solutions [17, 18]. Furthermore, the influence of bismuth addition on the microstructure and the properties of Sn-rich Sn–Ag lead-free solders has been also widely studied [13, 19–23]. However, the effect of bismuth on the corrosion behaviour in the case of micro-alloyed solder alloy is not deeply addressed in the literature. Therefore, this study was carried out corrosion investigations on lead-free micro-alloyed solder alloys. Finally, it was highlighted that the silver and bismuth content may pose a relative high corrosion risk related to micro-alloyed solder alloys used in electronics. The

reason could be that the corrosion potential (Ecorr) is shifted towards less noble values with the addition of bismuth and silver (See Table 2 and [18]).
To further and even deeper understand the effect of bismuth on the corrosion behaviour, the formed bismuth intermetallic phases and other intermetallic phases have to be investigated. The intermetallic phases have also an influence on the corrosion properties due to the different anodic dissolution rate comparing to the dissolution rates of the pure metals. Namely, the anodic dissolution rate has a significant impact on the corrosion rate as well.

Conclusion

The corrosion properties of different lead-free micro-alloyed solder alloys were investigated using a potentiodynamic polarization tests and SEM-EDS methods. According to the potentiodynamic polarization tests sample V showed highest critical current density and as well as the highest passivation current density (See Table 2), which means the bismuth-alloyed (3 wt%) solder alloy showed the weakest corrosion resistance. The corrosion depth results have confirmed that the bismuth bearing (3 wt%) lead-free solder alloy (sample V) have the lowest corrosion resistance compared to the other ones. The lower corrosion resistance can be explained by relevant silver and bismuth contents and volumes, which were detected in the corroded layers by energy dispersive spectroscopy. The reason could be that the corrosion potential (Ecorr) is shifted towards less noble values with the addition of bismuth and silver. So, it was shown that bismuth can have a significant impact on the corrosion behaviour related to Sn-based micro-alloyed solder alloys in 3.5 wt% NaCl solution. Therefore, it can be stated that (silver) and bismuth content may pose a relative high corrosion risk in case of micro-alloyed solder alloys as well.

References

[1] Directive of the European Commission for the Reduction of Hazardous Substances, Directive 2000/0159 (COD) C5-487/2002, LEX 391, PE-CONS 3662/2/02 Rev 2, ENV581, CODEC 1273, 2003.

[2] Miller, C.M., Anderson, IE., Smith, JF. "A viable Tin–lead solder substitute: Sn–Ag–Cu", Journal of Electronic Materials. 23. pp. 595–601. 1994. DOI: 10.1007/BF02653344

[3] Verdingovas, V., Jellesen, M. S., Ambat, R. "Impact of NaCl Contamination and Climatic Conditions on the Reliability of Printed Circuit Board Assemblies", IEEE Transactions on Device and Materials Reliability. 14(1). pp. 42-51. 2014. DOI: 10.1109/TDMR.2013.2293792

[4] Vimala, J. S., Natesan, M., Rajendran, S. "Corrosion and Protection of Electronic Components in Different Environmental Conditions - An Overview", The Open Corrosion Journal. 2. pp. 105-113. 2009. DOI:

[5] Zhong, X., Zhang, G., Qiu, Y., Chen, Z., Guo, X., Fu, C. "The corrosion of tin under thin electrolyte layers containing chloride", Corros Sci. 66. pp. 14-25. 2013. DOI: 10.1016/j.corsci.2012.08.040

[6] Law, C. M. T., Wu, C. M. L., Yu, D. Q. , Wang, L., Lai, J. K. L. "Microstructure, solderability, and growth of intermetallic compounds of Sn-Ag-Cu-RE lead-free solder alloys", J Electron Mater. 35(1). pp. 89-93. 2006. DOI: 10.1007/s11664-006-0189-7

[7] Krammer, O., Garami, T. "Reliability Investigation of Low Silver Content Micro-alloyed SAC Solders", In: 35th International Spring Seminar on Electronics Technology, ISSE, Salzburg, Austria, may 9-13, 2012. pp. 149-154. DOI: 10.1109/ISSE.2012.6273126

[8] Liu, Y., Sun, F., Zhang, H., Zou, P. "Solderability, IMC evolution, and shear behavior of low-Ag Sn0.7Ag0.5Cu-BiNi/Cu solder joint", J Mater Sci-Mater El. 3(9). pp. 1705-1710. 2012. DOI: 10.1007/s10854-012-0649-1

[9] Cheng, F., Gao, F., Zhang, J., Jin, W., Xiao, X. "Tensile properties and wettability of SAC0307 and SAC105 low Ag lead-free solder alloys", J Mater Sci-Mater El. 46(10). pp. 3424-3429. 2011. DOI: 10.1007/s10853-010-5231-8

[10] Fenglian, S., Yang, L., Jiabing, W. "Improving the solderability and electromigration behavior of Low-Ag SnAgCu soldering", In: 12th International Conference on Thermal, Mechanical and Multi-Physics Simulation and Experiments in Microelectronics and Microsystems, Linz, Austria, april 18-20 2011. pp. 1-5. DOI: 10.1109/ESIME.2011.5765807

[11] Medgyes, B., Tamási, P., Hajdu, F., Murányi, R., Lakatos-Varsányi, M., Gál, L., Harsányi, G. "Corrosion investigations on Lead-Free Micro-alloyed Solder Alloys used in Electronics", In: 38th International Spring Seminar on Electronics Technology, Eger, Hungary, may 6-10, 2015. pp. 296-299. DOI: 10.1109/ISSE.2015.7248009

[12] Hansen, K. S., Jellesen, M. S., Møller, P., Westermann, P. J. S., Ambat, R. "Effect of Solder Flux Residues on Corrosion of Electronics", Reliability and Maintainability Symposium, Fort Worth, TX, 26-29 Jan. 2009. pp. 502-508. DOI: 10.1109/RAMS.2009.4914727

[13] Huang, M.L., Wang, L. Metall. "Effects of Cu, Bi, and In on microstructure and tensile properties of Sn-Ag-X(Cu, Bi, In) solders", Mater. Trans. A. 36(6). pp. 1439-1446. 2005. DOI: 10.1007/s11661-005-0236-7

[14] Hassam, S., Dichi, E., Legendre, B. "Experimental equilibrium phase diagram of the Ag–Bi–Sn system" J. Alloys Compd. 268(1). pp. 199-206. 1998. DOI: 10.1016/S0925-8388(97)00617-8

[15] Huang, M.L., Wu, C.M.L., Lai, J.K.L., Chan, Y.C. "Microstructural evolution of a lead-free solder alloy Sn-Bi-Ag-Cu prepared by mechanical alloying during thermal shock and aging" J. Electron. Mater. 29(8). pp. 1021-1026. 2000. DOI: 10.1007/s11664-000-0167-4

[16] Ochoa, F., Williams, J.J., Chawla, N. "Effects of cooling rate on the microstructure and tensile behavior of a Sn-3.5wt.%Ag solder" J. Electron. Mater. 32(12). pp. 1414-1420. 2003. DOI: 10.1007/s11664-003-0109-z

[17] Rosalbino, F., Angelini, E., Zanicchi G., Marazza R. "Corrosion behaviour assessment of lead-free Sn–Ag–M (M = In, Bi, Cu) solder alloys", Materials Chemistry and Physics. 109. pp. 386-391. 2008. DOI: 10.1016/j.matchemphys.2007.12.006

[18] Ahmido A., Sabbar, A., Zouihri, H., Dakhsi, K., Guedira, F., Serghini-Idrissi, M., El Hajjaji, S. "Effect of bismuth and silver on the corrosion behavior of Sn–9Zn alloy in NaCl 3 wt.% solution", Materials Science and Engineering: B, 176(13). pp. 1032-1036. 2011. DOI: 10.1016/j.mseb.2011.05.034

[19] Vianco, P.T., Rejent, J.A. "Properties of ternary Sn-Ag-Bi solder alloys: Part II—Wettability and mechanical properties analyses", J. Electron. Mater. 28 (11). pp. 1138-1143. 1999. DOI: doi:10.1007/s11664-999-0251-3

[20] Moser, Z., Gasior, W., Pstrus, J. "Surface tension measurements of the Bi-Sn and Sn-Bi-Ag liquid alloys", J. Electron. Mater. 30 (9). pp. 1104-1111. 2001. DOI: 10.1007/s11664-001-0136-6

[21] Hwang, C.W., Suganuma, K. "Joint reliability and high temperature stability of Sn–Ag–Bi lead-free solder with Cu and Sn–Pb/Ni/Cu substrates", Mater. Sci. Eng. A. 373(1). pp. 187-194. 2004. DOI: 10.1016/j.msea.2004.01.019

[22] He, M., Acoff, V.L. "Effect of reflow and thermal aging on the microstructure and microhardness of Sn-3.7Ag-xBi solder alloys", J. Electron. Mater. 35(12). pp. 2098-2106. 2006. DOI: 10.1007/s11664-006-0319-2

[23] Anderson, E. "Development of Sn–Ag–Cu and Sn–Ag–Cu–X alloys for Pb-free electronic solder applications" J. Mater. Sci. Electron. 18(1). pp. 55-76. 2007. DOI: 10.1007/s10854-006-9011-9

A fent közölt kutatási eredmények publikálásra kerültek:

Patrik Tamási, György Kósa, Bence Szabó, Richárd Berényi, Bálint Medgyes
Effect of Bismuth and Silver on the Corrosion Behavior of Lead-free Solders in 3.5 wt% NaCl Solution
***PERIODICA POLYTECHNICA-ELECTRICAL ENGINEERING AND COMPUTER SCIENCE* 60:**(4) pp. 232-236. (2016)
DOI, Teljes dokumentum

Készítette: Szabó Bence

Budapest, 2017. január 05.